

Percolation on branching simplicial and cell complexes and its relation to interdependent percolation

Ginestra Bianconi

*School of Mathematical Sciences, Queen Mary University of London, London, E1 4NS, United Kingdom
The Alan Turing Institute, The British Library, London NW1 2DB, United Kingdom*

Ivan Kryven

Mathematical Institute, Utrecht University, PO Box 80010, 3508 TA Utrecht, the Netherlands

Robert M. Ziff

*Center for the Study of Complex Systems and Department of Chemical Engineering,
University of Michigan, Ann Arbor, Michigan 48109-2800, USA*

Network geometry has strong effects on network dynamics. In particular, the underlying hyperbolic geometry of discrete manifolds has recently been shown to affect their critical percolation properties. Here we investigate the properties of link percolation in non-amenable two-dimensional branching simplicial and cell complexes, i.e., simplicial and cell complexes in which the boundary scales like the volume. We establish the relation between the equations determining the percolation probability in random branching cell complexes and the equation for interdependent percolation in multiplex networks with inter-layer degree correlation equal to one. By using this relation we show that branching cell complexes can display more than two percolation phase transitions: the upper percolation transition, the lower percolation transition, and one or more intermediate phase transitions. At these additional transitions the percolation probability and the fractal exponent both feature a discontinuity. Furthermore, by using the renormalization group theory we show that the upper percolation transition can belong to various universality classes including the Berezinskii-Kosterlitz-Thouless (BKT) transition, the discontinuous percolation transition, and continuous transitions with anomalous singular behavior that generalize the BKT transition.

I. INTRODUCTION

Understanding the interplay between network structure and dynamics [1] has been a fundamental research question in statistical mechanics of networks [2, 3]. Recently this field has gained much momentum thanks to the vibrant research on generalized network structures, including multilayer networks [4–6] and simplicial and cell complexes [7–18]. In particular the study of percolation [19, 20] on generalized network structures has renewed interest to the so-called *explosive phenomena* [21], which have been investigated for single networks [22–26] as well as in the context of interdependent percolation in multilayer networks [4, 27–31] and percolation in hyperbolic simplicial and cell complexes [12, 13, 32]. Multilayer networks include links representing interactions of different natures and connotations. As such, multilayer networks can describe interacting networks as diverse as global infrastructures, financial systems, and the brain. In the last years it has been shown [4, 27] that interdependent percolation of multilayer networks leads to discontinuous phase transitions, revealing their intrinsic fragility. Simplicial and cell complexes are built using geometrical building blocks comprising of triangles, polygons and polytopes. As such they are ideal generalized network structures to investigate the interplay between hyperbolic network geometry and dynamics [9, 12, 13, 32–35]. Recently it has been found [32] that link percolation in hyperbolic Farey graphs and some well-behaved two-dimensional hyperbolic manifolds con-

stituting the skeleton of cell complexes [13] is discontinuous. Despite the fact that both percolation on simplicial and cell complexes and interdependent percolation in multilayer networks can lead to discontinuous phase transitions, the relation between the two critical phenomena has not been so far investigated.

In this paper we depart from the study of discrete manifolds and we consider branching simplicial and cell complexes that reduce in some limit to very well-studied hierarchical network structures, as for instance, the flower network and its generalizations [36–39]. These branching simplicial and cell complexes display a critical behavior of percolation that can be fully characterized using the renormalization group (RG) [13, 40–45]. Interestingly, our RG investigation of branching simplicial and cell complexes reveals a surprising relation between percolation in these structures and interdependent percolation on multilayer networks. Namely, we uncover a mathematical mapping between the equation determining the percolation probability in some specific simplicial and cell complexes and the equation determining the emergence of the Mutually Connected Giant Component (MCGC) [4, 27] of correlated and interdependent multiplex networks [46]. These correlated multiplex networks have recently been shown to be able to sustain multiple phase transitions [46]. Building upon the revealed mathematical mapping between the percolation in branching cell complexes and interdependent percolation, we are able to show that branching simplicial and cell complexes are not only characterized by their upper and lower per-

colation thresholds, as is the general rule for all non-amenable graphs [47], but they can feature intermediate phase transitions as well. These intermediate percolation transitions are discontinuous and can be observed when the distribution r_k , which denotes the probability that a randomly chosen link branches into k m -polygons, is multi-modal.

Moreover, in this paper we identify the conditions that guarantee a non-trivial discontinuous percolation transition at the upper percolation threshold of two-dimensional simplicial and cell complexes. Using the RG technique we show that as the topology of the branching simplicial and cell complexes changes, it is possible to observe a change of universality class of percolation between the discontinuous and Berezinskii-Kosterlitz-Thouless (BKT) phase transitions, confirming and generalizing the results in Refs. [36–39]. Moreover, we show that the system might display higher-order critical points corresponding to continuous transitions with non-trivial singular behavior, which, to our knowledge, has not been reported previously on similar structures.

The paper is structured as follows: in Sec. II we define the branching simplicial and cell complexes considered in this paper; in Sec. III we characterize their percolation probability; in Sec. IV we reveal the relation with interdependent percolation of correlated multiplex networks; in Sec. V we show that simplicial and cell complexes can undergo more than two percolation phase transitions; in Sec. VI we derive the expression of the generating function of the cluster-size distribution; in Sec. VII we derive the expression and the critical behavior of the fractal exponent, and in Sec. VIII we use the RG approach to predict the nature of the percolation transition at the upper percolation threshold. Finally in Sec. IX we provide the conclusions.

II. BRANCHING SIMPLICIAL AND CELL COMPLEXES

Hierarchical networks with a non-amenable structure can be manifolds, or more generally, branching simplicial and cell complexes. Here we focus on a few specific examples of two-dimensional branching simplicial and cell complexes. A two-dimensional simplicial complex is a topological structure formed by gluing triangles along their links, whereas a two-dimensional cell complex generalizes this concept by gluing arbitrary m -polygons along their links. Two-dimensional simplicial and cell complexes form manifolds only if each link is incident to at most two triangles (for the simplicial complexes) or two polygons (for the cell complexes). However, if this condition is not satisfied, the resulting topological structures are not discrete manifolds. A branching hierarchical simplicial complex or cell complex is a network that can be constructed by successively gluing triangles or polygons to single links such that each link can be incident to more than two polygons. Probably the most

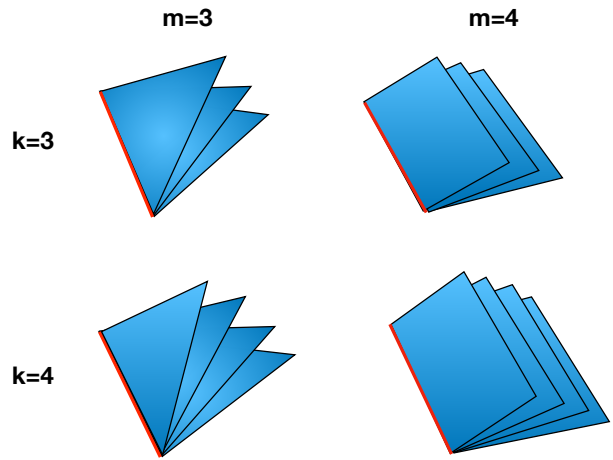


FIG. 1. We show the first iteration $n = 1$ of the branching process in which the initial single link (shown as a thick red line) branches out to k , m -polygons with k drawn from the distribution r_k . Here the first iteration is shown for different values of $m = 3, 4$ (corresponding to the attachment of triangles and rectangles respectively) and $k = 3, 4$.

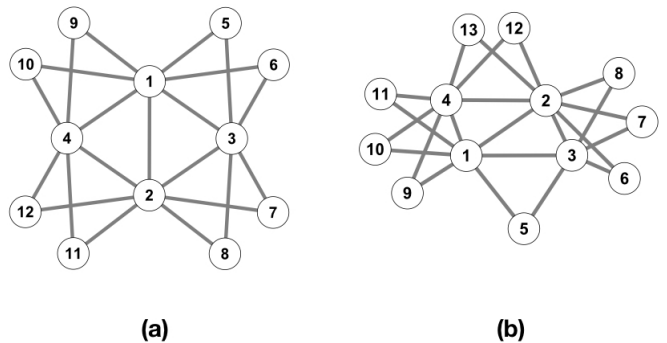


FIG. 2. The result of the first $n = 2$ iterations are shown for: (a) the flower network with $m = 3$ and $r_k = \delta_{k,2}$, and (b) for a random branching cell complex with $m = 3$ with non-zero probabilities r_1, r_2, r_3 . In both cases nodes 1, 2 are the nodes present at the iteration $n = 0$, nodes 3, 4 are the nodes added at the iteration $n = 1$, and all the other nodes are added at iteration $n = 2$.

discussed hierarchical branching simplicial complex is the flower network which stems from the Migdal-Kadanoff [48, 49] renormalization group techniques. Here we focus on the percolation properties of branching simplicial and cell complexes that feature random and deterministic structure and generalize the flower network as described below.

A branching tree can be constructed by starting at iteration $n = 0$ from a single node. At every time $n > 0$ the node connected to a single link is connected to k new links with probability r_k . This construction can be generalized to random branching cell complexes in dimension

$d = 2$. We start at iteration $n = 0$ from a single initial link. At iteration $n = 1$ we attach a $k \geq 1$ polygons with m faces (m -polygons) to it with k drawn from the probability distribution r_k (see Fig. 1). At iteration $n > 1$, we glue $k \geq 1$ new m -polygons with probability r_k to each link introduced at iteration $n - 1$. In this way, the number of polygons k is treated as a random variable.

At iteration n the average number of nodes \bar{N}_n and links \bar{L}_n is given by

$$\bar{N}_n = 2 + \frac{\langle k \rangle (m - 2)}{\langle k \rangle (m - 1) - 1} [\langle k \rangle^n (m - 1)^n - 1], \quad (1)$$

$$\bar{L}_n = \frac{1}{\langle k \rangle (m - 1) - 1} [\langle k \rangle^{n+1} (m - 1)^{n+1} - 1]. \quad (2)$$

In the case $m = 3$ the polygons are triangles, and the same iterative process generates a random branching simplicial complex. Here we refer to networks with arbitrary fixed $m \geq 3$ as simply the cell complexes. We note that the case $m = 3$ and $r_k = \delta_{k,2}$ corresponds to the flower network shown in Fig. 2a. A branching cell complex with $m = 3$ and heterogeneous r_k distribution is shown in Fig. 2b.

III. PERCOLATION IN NON-AMENABLE NETWORK STRUCTURES

We consider link percolation on branching cell complexes where we remove each link independently with probability $q = 1 - p$. Since the random branching cell complexes that we consider are non-amenable structures [47], link percolation displays at least two percolation thresholds. In particular, as in hyperbolic manifolds [12, 13, 32], we distinguish between the lower p^* and the upper p_c percolation thresholds leading to the identification of three distinct phases.

- (1) For $p < p^*$, i.e., below the lower percolation threshold, there is no infinite cluster. Therefore the percolation probability, i.e., the probability that the two initial nodes are connected at least by a path of non-damaged nodes, is $T = 0$.
- (3) For $p^* < p < p_c$ the percolation probability $0 < T < 1$ and M_n , the number of nodes in the largest component at iteration n , is subextensive, i.e.,

$$M_n = (\bar{N}_n)^{\psi_n}, \quad (3)$$

where the limit of the exponent ψ_n for $n \rightarrow \infty$, i.e.,

$$\psi = \lim_{n \rightarrow \infty} \psi_n \quad (4)$$

is called the *fractal exponent*. In this phase we have $\psi < 1$.

- (3) For $p > p_c$, i.e., above the upper percolation threshold, there is an infinite cluster which is extensive.

This implies that the percolation probability $T = 1$ and $\psi = 1$. Moreover, if we indicate with M_n the number of nodes in the largest component at iteration n above the upper percolation threshold, the fraction of nodes in the largest component $P_\infty(p)$ is of order one, i.e.,

$$P_\infty(p) = \lim_{n \rightarrow \infty} \frac{M_n}{N_n} = O(1). \quad (5)$$

IV. PERCOLATION PROBABILITY

In this section we investigate the percolation probability T_n indicating the probability that the two nodes present at iteration $n = 0$ are connected with a path within the first n iterations.

The percolation probability T_n for the random branching cell complexes satisfies the following recursive equation

$$T_{n+1} = 1 - (1 - p) \sum_{k \geq 1} r_k (1 - T_n^{m-1})^k, \quad (6)$$

That is, the two initial nodes are not connected at iteration $n + 1$ if the link that connects the initial nodes is removed and there is no path connecting these nodes through the m -polygons within the first n iterations. In the limit of an infinite network, $n \rightarrow \infty$, the linking probability T_n converges to the percolation probability T , i.e., $T_n \rightarrow T$, where T satisfies

$$T = 1 - (1 - p) \sum_{k \geq 1} r_k (1 - T^{m-1})^k. \quad (7)$$

Note that in presence of multiple solutions of Eq. (7) we only consider the solution $T \in [0, 1]$ with the smallest value. By defining $R(z)$ as the generating function of the distribution r_k , i.e.,

$$R(z) = \sum_{k \geq 1} r_k z^k, \quad (8)$$

and by defining $Q(T)$ as

$$Q(T) = T^{m-1}, \quad (9)$$

we can write Eq. (7) as

$$f(T) = T - 1 + (1 - p)R(1 - Q(T)) = 0. \quad (10)$$

A close inspection of this equation reveals important properties of the critical behavior of the random branching cell complexes. We first observe that $T = 0$ is a solution of Eq. (10) only for $p = 0$. Therefore it follows that the lower percolation threshold p^* is given by

$$p^* = 0, \quad (11)$$

for every branching cell complex studied in this work.

Secondly we will show that applying the theory of critical phenomena, we can obtain information on the other

possible percolation thresholds that can be encountered at discontinuous hybrid critical points, second-order critical points, and higher-order critical points of Eq. (10). The discontinuous hybrid critical point, also called the *saddle-node bifurcation*, is found by imposing $T_c < 1$ and

$$\begin{aligned} f(T_c)|_{p=p_c} &= 0, \\ f'(T_c)|_{p=p_c} &= 0, \\ f''(T_c)|_{p=p_c} &< 0. \end{aligned} \quad (12)$$

If the above equations yield many solutions (p_c, T_c) one has to select a subset that forms a minimal subsequence that is simultaneously ascending in both variables p_c and T_c . In order to find the critical behavior of ΔT let us expand Eq. (10) close to this critical point characterized by $|\Delta T| = |T - T_c| \ll 1$ and $|\Delta p| = |p - p_c| \ll 1$ and $\Delta p < 0, \Delta T < 0$. In this way we get

$$\begin{aligned} 0 = & f(T_c)|_{p=p_c} + f'(T_c)|_{p=p_c} \Delta T + \frac{\partial f(T_c)}{\partial p} \Big|_{p=p_c} \Delta p \\ & + \frac{\partial^2 f(T_c)}{\partial p \partial T} \Big|_{p=p_c} \Delta p \Delta T + \frac{1}{2} \frac{\partial^2 f(T_c)}{\partial T^2} \Big|_{p=p_c} (\Delta T)^2 + \dots \end{aligned}$$

Since $T_c < 1$ we have $\partial f(T_c)/\partial p|_{p=p_c} < 0$. Therefore, for $|\Delta T| = |T - T_c| \ll 1$ and $|\Delta p| = |p - p_c| \ll 1$ with $\Delta p < 0, \Delta T < 0$, we have the hybrid critical behavior

$$\hat{A} \Delta p \simeq (\Delta T)^2, \quad (13)$$

or equivalently

$$|\Delta T| \simeq |\hat{A} \Delta p|^\beta, \quad (14)$$

where

$$\beta = \frac{1}{2}, \quad (15)$$

and

$$\hat{A} = - \left[\frac{\partial f(T_c)}{\partial p} \Big|_{p=p_c} \right] \left[\frac{1}{2} \frac{\partial^2 f(T_c)}{\partial T^2} \Big|_{p=p_c} \right]^{-1}. \quad (16)$$

The second-order critical point, also called the *transcritical bifurcation*, is characterized by the following conditions on $f(T)$

$$\begin{aligned} f(1)|_{p=p_c} &= 0, \\ f'(1)|_{p=p_c} &= 0, \\ f''(1)|_{p=p_c} &< 0. \end{aligned} \quad (17)$$

In this way we find the critical point (p_c, T_c) with

$$\begin{aligned} p_c &= 1 - \frac{1}{(m-1)r_1}, \\ T_c &= 1, \end{aligned} \quad (18)$$

obtained as long as there is no discontinuous critical point for $p < 1 - 1/[(m-1)r_1]$ and provided that

$$r_1 > \max \left[\frac{1}{m-1}, 2 \frac{m-1}{m-2} r_2 \right]. \quad (19)$$

In order to find the critical behavior of ΔT let us expand Eq. (10) close to this critical point characterized by $|\Delta T| = |T - 1| \ll 1$ and $|\Delta p| = |p - p_c| \ll 1$ and $\Delta p < 0, \Delta T < 0$. By taking into account the critical point conditions expressed in Eq. (17) and the fact that $\partial f(T_c)/\partial p|_{p=p_c} = 0$ because $T_c = 1$, for $\Delta p < 0$ the expansion gives the mean-field behavior

$$\Delta T \simeq (A \Delta p)^\beta, \quad (20)$$

where

$$\beta = 1, \quad (21)$$

and

$$A = - \left[\frac{\partial^2 f(T_c)}{\partial p \partial T} \Big|_{p=p_c} \right] \left[\frac{1}{2} \frac{\partial^2 f(T_c)}{\partial T^2} \Big|_{p=p_c} \right]^{-1}. \quad (22)$$

In a model of random branching cell complexes with arbitrary distribution r_k , the manifold of second-order critical points meets the manifolds of hybrid transitions on a set of tricritical points. The tricritical points of Eq. (10), also called the *pitchfork bifurcation* points, can be found by imposing the conditions

$$\begin{aligned} f(1)|_{p=p_c} &= 0, \\ f'(1)|_{p=p_c} &= 0, \\ f''(1)|_{p=p_c} &= 0, \\ f'''(1)|_{p=p_c} &> 0. \end{aligned} \quad (23)$$

These equation identify the tricritical point (p_c, T_c) , which is given by

$$\begin{aligned} p_c &= 1 - \frac{1}{(m-1)r_1}, \\ T_c &= 1, \end{aligned} \quad (24)$$

as long as there is no discontinuous transition for $p < 1 - 1/[(m-1)r_1]$ and provided that

$$r_1 = 2 \frac{m-1}{m-2} r_2 \quad (25)$$

where

$$r_1 > \max \left[\frac{1}{m-1}, 6 \frac{(m-1)^2}{(2m-3)(m-2)} r_3 \right]. \quad (26)$$

We expand Eq. (10) close to the critical point for $|\Delta T| = |T - 1| \ll 1$ and $|\Delta p| = |p - p_c| \ll 1$ up to third order. We observe that since $T_c = 1$ we have $\partial f(T_c)/\partial p|_{p=p_c} = 0$. Therefore for $\Delta p < 0$ we obtain the tricritical scaling

$$\tilde{A} \Delta p \simeq (\Delta T)^2, \quad (27)$$

or equivalently

$$|\Delta T| \simeq |\tilde{A} \Delta p|^\beta, \quad (28)$$

where

$$\beta = \frac{1}{2}, \quad (29)$$

and

$$\tilde{A} = - \left[\frac{\partial^2 f(T_c)}{\partial p \partial T} \Big|_{p=p_c} \right] \left[\frac{1}{3!} \frac{\partial^3 f(T_c)}{\partial T^3} \Big|_{p=p_c} \right]^{-1}. \quad (30)$$

Similarly it is possible to observe even higher-order critical points of order $s > 3$. Such *higher-order pitchfork bifurcations* are characterized by

$$f^{(j)}(1) \Big|_{p=p_c} = 0, \quad (31)$$

for $j = 0, 1, 2, \dots, s-1$ and

$$(-1)^{s-1} f^{(s)}(1) \Big|_{p=p_c} > 0. \quad (32)$$

Consequently these higher-order critical points are observed when

$$r_k = \frac{\Gamma\left(k - \frac{1}{m-1}\right)}{\Gamma\left(1 - \frac{1}{m-1}\right) \Gamma(k+1)} r_1 \quad (33)$$

for $k = 2, \dots, s-1$, and

$$r_1 > \max \left[\frac{1}{m-1}, \frac{\Gamma\left(1 - \frac{1}{m-1}\right) \Gamma(s)}{\Gamma\left(s - \frac{1}{m-1}\right)} r_s \right]. \quad (34)$$

These transitions occur at

$$p_c = 1 - \frac{1}{(m-1)r_1}$$

as long as there are no discontinuous critical points for $p < 1 - 1/[(m-1)r_1]$. At a critical point of order s we observe the critical scaling

$$|\Delta T| \simeq |\tilde{A}_s \Delta p|^\beta, \quad (35)$$

where

$$\beta = \frac{1}{s-1},$$

and \tilde{A}_s is given by

$$\tilde{A}_s = - \left[\frac{\partial^2 f(T_c)}{\partial p \partial T} \Big|_{p=p_c} \right] \left[\frac{1}{(s+1)!} \frac{\partial^s f(T_c)}{\partial T^s} \Big|_{p=p_c} \right]^{-1},$$

Finally, in the limiting case of $s \rightarrow \infty$, the critical exponent β vanishes and T features a 0-to-1 discontinuity at $p_c = 0$.

V. MATHEMATICAL MAPPING TO INTERDEPENDENT PERCOLATION IN DEGREE-CORRELATED MULTIPLEX NETWORKS

The equation determining the percolation probability in random branching cell complexes can be related to

Branching Cell-Complex	Correlated Multiplex Network
T	$1 - S'$
p	$1 - \tilde{p}$
m	$\kappa + 1$
r_k	$P(B)$

TABLE I. Mathematical mapping between the quantities determining the percolation probability T in the modified branching cell complex and the mathematical quantities determining the probability S' that by following a random link of a random correlated multiplex network with activity distribution $P(B)$ and homogeneous degree of each replica node $\kappa = m - 1$ we reach a node in the MCGC.

the equations determining the MCGC in a correlated multiplex network. However, in order to perform an exact mathematical mapping between the two problems and their corresponding equations, one should consider a slight modification of the original model of random branching cell complexes. Consider the modified branching cell complex model with $m \geq 3$ in which we break the symmetry between the k polygons attached to any given link and impose a maximum value k_{max} . The modified model is defined iteratively as in the following. We start at iteration $n = 0$ from a single initial link. At iteration $n \geq 1$ to each link introduced at iteration $n - 1$ we glue $(k - 1)$ m -polygons and one $(m - 1)$ -polygon to it with $k \geq 1$ drawn from the probability distribution r_k . For this modified random branching cell complex model, the probability that the two initial nodes are connected at iteration n when links are removed with probability $q = 1 - p$ is given by

$$T_{n+1} = 1 - (1 - p) \sum_{k \geq 1} r_k (1 - T_n^{m-2}) (1 - T_n^{m-1})^{k-1},$$

and for large network sizes, when $n \rightarrow \infty$, we have

$$T = 1 - (1 - p) \sum_{k \geq 1} r_k (1 - T^{m-2}) (1 - T^{m-1})^{k-1}.$$

This equation can be exactly mapped to the equation determining the probability S' that by following a link we reach a node in the MCGC of a multiplex network with heterogeneous activities of the nodes and maximum correlation between the degree of the nodes in different layers. In fact, let us consider a multiplex network [4] of \hat{M} layers in which all replica nodes (i, α) in an arbitrary layer $\alpha = 1, 2, \dots, \hat{M}$ have the same activity $B_i = B_i^{[\alpha]}$ indicating the number of replica nodes that are interdependent to it and have the same degree $\kappa = \kappa_i^{[\alpha]}$ which is independent of the node i and of the layer α . In this highly correlated multiplex network studied in Ref. [46] let us consider the MCGC when nodes are damaged with probability $1 - \tilde{p}$. The equation for the probability S' that by following a link of the multiplex network in a given layer α we reach a node in the MCGC reads

$$S' = \tilde{p} \sum_B P(B) [1 - (1 - S')^{\kappa-1}] [1 - (1 - S')^\kappa]^{B-1},$$

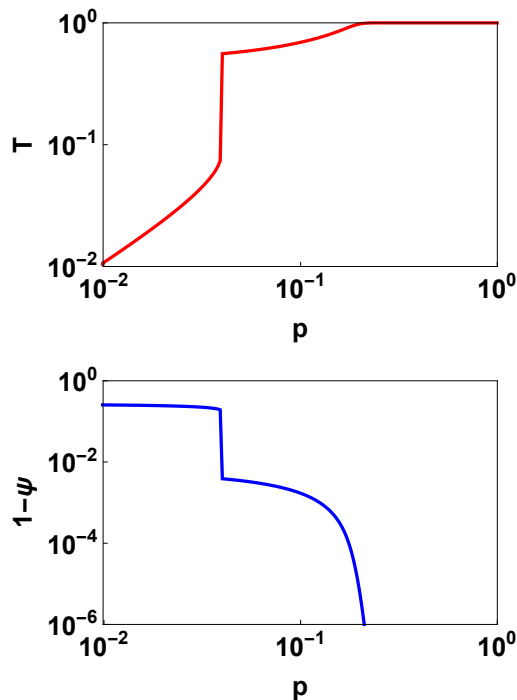


FIG. 3. The percolation probability T and $1 - \psi$ versus the occupation probability of the links p , where ψ is the fractal exponent. The considered branching simplicial complex ($m = 3$) has three percolation thresholds: the lower percolation threshold at $p^* = 0$, the upper percolation threshold at $p_c = 0.1935(5)$ and one intermediate percolation threshold at $p_c^* = 0.0395(6)$. At the intermediate percolation threshold both T and ψ have a discontinuity but remain smaller than one. Here the branching simplicial complex has $r_k = 0.62\delta_{k,1} + 0.07\delta_{k,2} + 0.31\delta_{k,20}$.

where $P(B)$ is the probability that a random node has activity $B_i = B$. At the mathematical level it is thus possible to define a mapping between the equation determining T in the modified random branching hyperbolic manifolds and the equation determining S' in the correlated multiplex network. In this mapping m corresponds to $\kappa + 1$, the probability distribution r_k corresponds to the activity distribution $P(B)$ and p corresponds to $1 - \tilde{p}$ (see Table I).

Since the considered multiplex networks have been shown to display multiple percolation phase transitions, it follows that the mapping described above suggests that also in the modified random branching network one may expect multiple critical points in the equation determining the linking probability. However, the question whether also in the originally considered random branching model we can expect multiple critical points of the linking probability needs to be explored in detail and will be addressed in the following section.

VI. MULTIPLE PERCOLATION TRANSITIONS

Here we provide evidence that random branching cell complexes can feature more percolation transitions in addition to the known upper and lower ones. These transitions can occur for $p = p_c^*$ with $p^* < p_c^* < p_c$ and they are characterized by discontinuities both in the percolation probability T and in the fractal exponent ψ , with $T < 1$ and $\psi < 1$ above and below the transition. In other words, the maximum cluster still remains sub-extensive after undergoing a discontinuous transition; see, for example, Fig. 3. These phase transitions correspond to hybrid critical points of Eq. (10) different from the upper or lower percolation threshold and correspond to the multiple percolation transitions observed in the correlated multiplex network considered in Ref. [46] for the modified branching network model. Here we investigate this interesting behavior in the context of a simplicial complex ($m = 3$) with a trimodal distribution r_k given by

$$r_k = r_1\delta_{k,1} + r_2\delta_{k,2} + \hat{r}\delta_{k,\hat{k}}, \quad (36)$$

where $r_1 + r_2 + \hat{r} = 1$ and $\hat{k} \geq 3$. By numerically studying the roots of Eq. (10) supplied with the trimodal distribution (36), we build the phase diagram of the model as a barycentric plot for various values of \hat{k} (see Fig. 4). In Fig. 4 we distinguish between different phases Ω_{ij} corresponding to parameter values for which the percolation probability displays $i = 0, 1, 2$ continuous, and $j = 0, 1, 2$ discontinuous and hybrid critical points, so that $i + j$ indicates the total number of distinct percolation thresholds. As shown in Fig 4 the phase diagram evolves when \hat{k} increases. Fig. 5 gives several examples of the percolation probability T as a function of p in the different phases and demonstrates the existence of intermediate percolation transitions. When $k \rightarrow \infty$, the phase diagram degenerates, and the phase diagram consists of three phases; see Fig. 6. In this limit we observe a phase Ω_{01} with a discontinuous 0-to-1 transition for the percolation probability T at $p^* = p_c = 0$. Interestingly by having a multi-modal r_k distribution and a random multi-modal distribution q_m of the number of sides of the polygons (with more than three modes) it is possible to observe even more than one intermediate phase transition (see for instance corresponding phenomenology in correlated multiplex networks described in Ref. [46]).

VII. GENERATING FUNCTION

Here we investigate the properties of the generating functions $\hat{T}_n(x)$ and $\hat{S}_n(x, y)$ that will be essential to characterize the different phases of percolation in the branching simplicial and cell complexes under investigation. The function $\hat{T}_n(x)$ is the generating function of the number of nodes in the connected component linked to both initial nodes of the considered random branching network. The function $\hat{S}_n(x, y)$ is the generating function

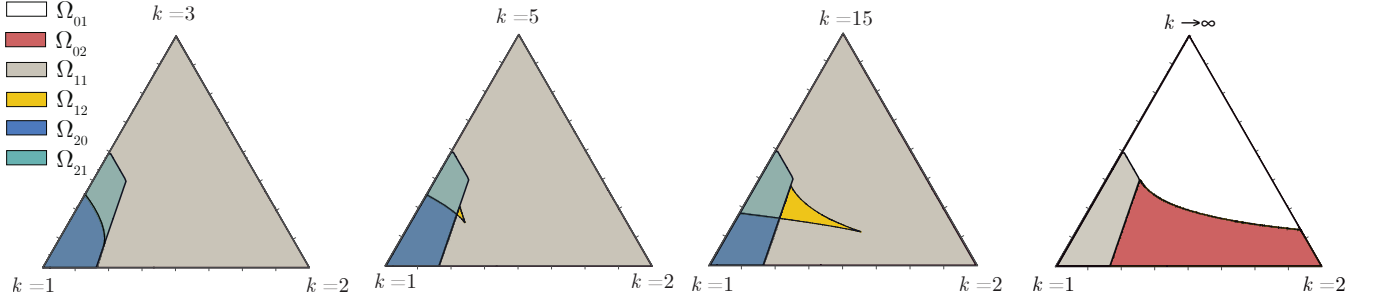


FIG. 4. The barycentric plot characterizing the phase diagram of link percolation for the branching simplicial complex with $m = 3$ and $r_k = r_1\delta_{k,1} + r_{k,2}\delta_{k,2} + r_{\hat{k}}\delta_{k,\hat{k}}$ where $\hat{k} = 3, 5, 15$, or is diverging. The parameter space $(r_1, r_2, r_{\hat{k}})$ is partitioned into phases Ω_{ij} at which the percolation probability T has i continuous and j discontinuous transitions. When $k \rightarrow \infty$ in the rightmost barycentric plot, the first two critical points merge and the domains $\Omega_{21}, \Omega_{11}, \Omega_{12}$ switch correspondingly to $\Omega_{11}, \Omega_{01}, \Omega_{02}$.

for the sizes of the two connected components linked exclusively to one of the two initial nodes of the same network. These generating functions are given by

$$\begin{aligned}\hat{T}_n(x) &= \sum_{\ell=0}^{\infty} t_n(\ell) x^\ell, \\ \hat{S}_n(x, y) &= \sum_{\ell=0}^{\infty} \sum_{\bar{\ell}=0}^{\infty} s_n(\ell, \bar{\ell}) x^\ell y^{\bar{\ell}},\end{aligned}\quad (37)$$

where $t_n(\ell)$ indicates the distribution of the number of nodes ℓ connected to the two initial nodes and $s_n(\ell, \bar{\ell})$ indicates the joint distribution of the number of nodes ℓ connected exclusively to a given initial node and the number of nodes $\bar{\ell}$ connected exclusively to the other initial node. By being guided by the diagrammatic representation of these quantities, as explained in Refs. [13, 32], we obtain the recursive equations for $\hat{T}_n(x)$ and $\hat{S}_n(x, y)$ that start from the initial condition $T_0(x) = 1 - \hat{S}_0(x, y) = p$ and read

$$\begin{aligned}\hat{S}_{n+1}(x, y) &= (1-p) \sum_{k=1}^{\infty} r_k \left[\sum_{r=0}^{m-2} x^r y^{m-2-r} \hat{T}_n^r(x) \hat{S}_n(x, y) \hat{T}_n^{m-2-r}(y) + \sum_{s=0}^{m-3} \sum_{r=0}^s x^r y^{s-r} \hat{T}_n^r(x) \hat{S}_n(x, 1) \hat{S}_n(y, 1) \hat{T}_n^{s-r}(y) \right]^k, \\ \hat{T}_{n+1}(x) &= \sum_{k=1}^{\infty} r_k \left[x^{m-2} \hat{T}_n^{m-1}(x) + (m-1) x^{m-2} \hat{T}_n^{m-2}(x) S_n(x, x) + \sum_{s=0}^{m-3} (s+1) x^s \hat{T}_n^s(x) \hat{S}_n(x, 1) \hat{S}_n(1, x) \right]^k \\ &\quad - (1-p) \sum_{k=1}^{\infty} r_k \left[(m-1) x^{m-2} \hat{T}_n^{m-2}(x) S_n(x, x) + \sum_{s=0}^{m-3} (s+1) x^s \hat{T}_n^s(x) \hat{S}_n(x, 1) \hat{S}_n(1, x) \right]^k, \end{aligned}\quad (38)$$

VIII. FRACTAL EXPONENT

A. General framework

The total number of nodes M_n that at iteration n are in the component connected to the two initial nodes can be obtained by differentiating the generating function $\hat{T}_n(x)$ i.e.,

$$M_n = \left. \frac{d\hat{T}_n(x)}{dx} \right|_{x=1}. \quad (39)$$

By following the mathematical framework proposed in Ref. [32] we rewrite Eqs. (38) in the vector form

$$\begin{aligned}\mathbf{V}_n(x) &= (V_n^1(x), V_n^2(x), V_n^3(x))^{\top} \\ &= (\hat{T}_n(x), \Sigma_n(x), S_n(x))^{\top},\end{aligned}\quad (40)$$

where $\Sigma_n(x) = \hat{S}_n(x, x)$, and $S_n(x) = \hat{S}(1, x)$ and obtain the recursive equation

$$\mathbf{V}_{n+1}(x) = \mathbf{F}_n(\mathbf{V}_n(x), x). \quad (41)$$

These equations are differentiated to obtain

$$\frac{d\mathbf{V}_{n+1}(x)}{dx} = \sum_{j=0}^n \sum_{s=1}^3 \frac{\partial \mathbf{F}_j}{\partial V_j^s(x)} \frac{dV_j^s(x)}{dx} + \frac{\partial \mathbf{F}_n}{\partial x}, \quad (42)$$

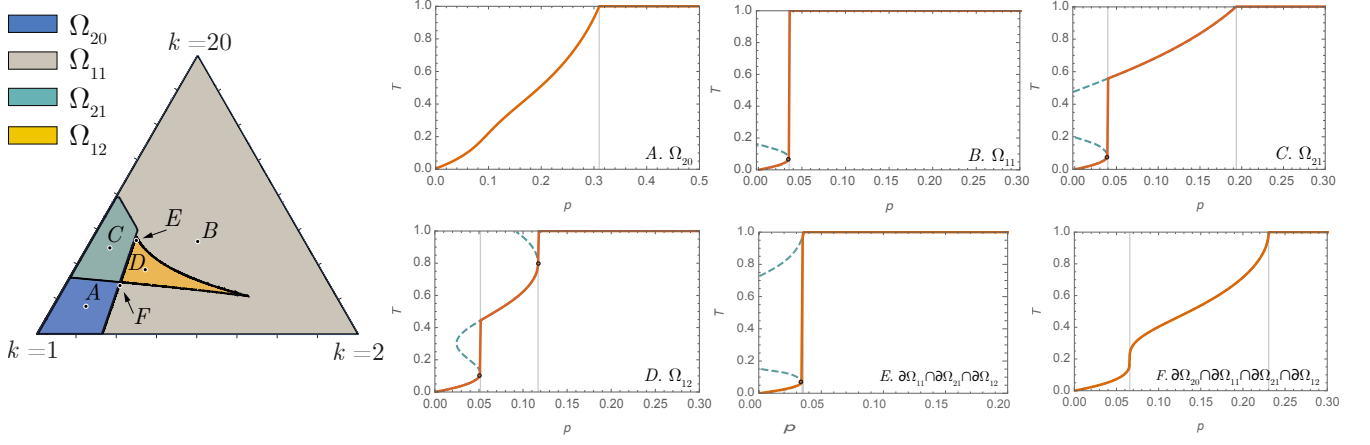


FIG. 5. The barycentric plot characterizing the phase diagram of link percolation for the branching simplicial complex with $m = 3$ and $r_k = r_1 \delta_{k,1} + r_2 \delta_{k,2} + r_{20} \delta_{k,20}$. The percolation probability T versus p is shown at points A, B, C, and D that belong to phases Ω_{20} , Ω_{21} , Ω_{21} and Ω_{12} respectively, at the shared accumulation points $E \in \Omega_{11} \cap \Omega_{21} \cap \Omega_{12}$, and $F \in \Omega_{20} \cap \Omega_{11} \cap \Omega_{21} \cap \Omega_{12}$. The sample points are given by the following barycentric coordinates (r_1, r_2, r_{20}) : $A = (0.8, 0.1, 0.1)$, $B = (0.33, 0.33, 0.33)$, $C = (0.62, 0.07, 0.31)$, $D = (0.55, 0.22, 0.23)$, $E = (0.52, 0.13, 0.35)$, and $F = (0.65, 0.16, 0.19)$. The dashed lines indicate the unstable branches and the vertical lines indicate the predicted positions of the discontinuous phase transitions.

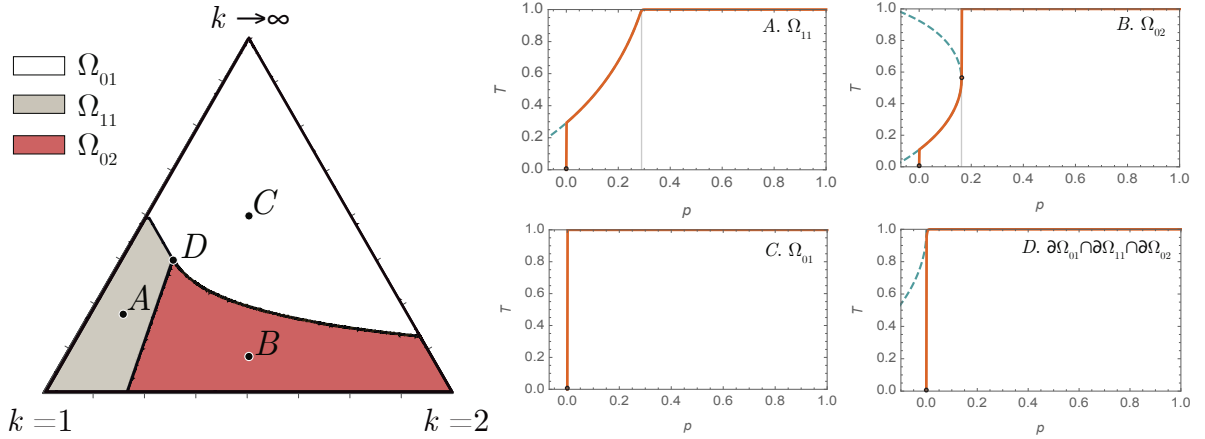


FIG. 6. The barycentric plot characterizing the phase diagram of link percolation for the branching simplicial complex with $m = 3$ and $r_k = r_1 \delta_{k,1} + r_2 \delta_{k,2} + r_\infty \delta_{k,\hat{k}}$ with $\hat{k} \rightarrow \infty$. The percolation probability T versus p is shown at points A, B, and C that belong to phases Ω_{11} , Ω_{02} , and Ω_{01} respectively, and at their shared accumulation point $D \in \Omega_{11} \cap \Omega_{01} \cap \Omega_{02}$. The sample points are given by their barycentric coordinates (r_1, r_2, r_∞) : $A = (0.70, 0.08, 0.22)$, $B = (0.45, 0.45, 0.1)$, $C = (0.25, 0.25, 0.50)$, and $D = (0.50, 0.13, 0.37)$. The dashed lines indicate the unstable branches and the vertical lines indicate the predicted positions of the discontinuous phase transitions.

with initial condition $\mathbf{V}'_0 = (0, 0, 0)$ (where we do not count the initial nodes).

We note that the non-homogeneous term $\partial \mathbf{F}_n / \partial x$ is subleading with respect to the homogeneous one. Therefore for $n \gg 1$ and $T < 1$, we can express M_n as

$$M_{n+1} \simeq \mathcal{D}_n \prod_{n'=1}^n \lambda_{n'} \mathbf{u}_{n'}, \quad (43)$$

where λ_n and \mathbf{u}_n are the largest eigenvalue and the corresponding eigenvector of the Jacobian matrix \mathbf{J}_n given

by

$$[J_n]_{ij} = \left. \frac{\partial F^i(x)}{\partial V^j(x)} \right|_{\mathbf{V}(x) = \mathbf{V}_n(1); x=1}, \quad (44)$$

and \mathcal{D}_n is given by

$$\mathcal{D}_n = \left(\prod_{n'=2}^n \langle \mathbf{u}_{n'} | \mathbf{u}_{n'-1} \rangle \right) \langle \mathbf{u}_1 | \dot{\mathbf{V}}_0 \rangle, \quad (45)$$

with $\dot{\mathbf{V}}_0 = \partial \mathbf{F}_0 / \partial x$. We will show that for $p \simeq p_c$, \mathcal{D}_n is in first approximation independent of n , therefore it

follows that $R_n = \dot{V}_n^1$ scales like

$$M_{n+1} \sim \prod_{n'=1}^n \lambda_{n'} = \exp \left[\sum_{n'=0}^n \ln \lambda_{n'} \right]. \quad (46)$$

By using Eq. (3) it follows that ψ_n is given by

$$\psi_n = \frac{\ln \lambda_n}{\ln[\langle k \rangle (m-1)]} \quad (47)$$

and the fractal exponent ψ can be calculated by performing the limit for $n \rightarrow \infty$, and using the definition of the fractal exponent given by Eq. (4).

B. Derivation of the fractal exponent ψ

In this section our goal is to derive the explicit expression for the fractal exponent ψ . From the explicit expression of the generating functions given by Eq. (38), we derive the closed equations for $\mathbf{V}_n = [\hat{T}_n(x), \Sigma_n(x), S_n(x)]^\top$, where $\Sigma_n(x) = \hat{S}_n(x, x)$, and $\hat{S}_n(x) = \hat{S}(1, x)$

$$\mathbf{V}_{n+1}(x) = \mathbf{F}(\mathbf{V}_n(x), x). \quad (48)$$

These equations read

$$\begin{aligned} \hat{T}_{n+1}(x) &= \sum_{k=1}^{\infty} r_k \left[x^{m-2} \hat{T}_n^{m-1}(x) + (m-1)x^{m-2} \hat{T}_n^{m-2}(x) \Sigma_n(x) + \left(\sum_{i=0}^{m-3} (i+1)x^i \hat{T}_n^i(x) \right) S_n^2(x) \right]^k \\ &\quad - (1-p) \sum_{k=1}^{\infty} r_k \left[(m-1)x^{m-2} \hat{T}_n^{m-2}(x) \Sigma_n(x) + \left(\sum_{i=0}^{m-3} (i+1)x^i \hat{T}_n^i(x) \right) S_n^2(x) \right]^k, \\ \Sigma_{n+1}(x) &= (1-p) \sum_{k=1}^{\infty} r_k \left[(m-1)x^{m-2} \hat{T}_n^{m-2}(x) \Sigma_n(x) + \left(\sum_{i=0}^{m-3} (i+1)x^i \hat{T}_n^i(x) \right) S_n^2(x) \right]^k, \\ S_{n+1}(x) &= (1-p) \sum_{k=1}^{\infty} r_k \left[\left(\sum_{i=0}^{m-2} x^i \hat{T}_n^i(x) \right) S_n(x) \right]^k. \end{aligned} \quad (49)$$

The Jacobian \mathbf{J}_n is obtained by differentiating Eq. (49) with respect to \mathbf{V}_n , by putting $x = 1$ and using $\hat{T}_n(1) = 1 - \Sigma_n(1, 1) = 1 - S_n(1) = T_n$. In order to perform this analytical calculation we have used the mathematical

identities

$$\begin{aligned} (1 - T_n) \sum_{i=0}^{m-3} i(i+1) T_n^{i-1} &= 2 \sum_{i=0}^{m-3} (i+1) T_n^i \\ &\quad - (m-1)(m-2) T_n^{m-3} \end{aligned} \quad (50)$$

and

$$(1 - T_n) \sum_{i=0}^{m-3} (i+1) T_n^i = \sum_{i=0}^{m-2} T_n^i - (m-1) T_n^{m-2}.$$

In this way it is easy to show that the Jacobian \mathbf{J}_n can be expressed as

$$\mathbf{J}_n = \begin{pmatrix} \langle k \rangle [2H(T_n) - Q'(T_n)] - 2(1-p)G(T_n) & Q'(T_n)[\langle k \rangle - (1-p)R'(1 - T_n^{m-1})] & 2[\langle k \rangle (H(T_n) - Q'(T_n)) - (1-p)G(T_n)] \\ 2(1-p)G(T_n) & (1-p)R'(1 - T_n^{m-1})Q'(T_n) & 2(1-p)G(T_n) \\ (1-p)G(T_n) & 0 & (1-p)R'(1 - T_n^{m-1})H(T_n) \end{pmatrix},$$

where $Q(T)$ is defined in Eq. (9) and $H(T)$ is defined as

$$H(T) = \sum_{i=0}^{m-2} T^i, \quad (51)$$

which admits for $T < 1$ the expression

$$H(T) = \frac{1 - Q(T)}{1 - T}. \quad (52)$$

Furthermore, $R'(z)$ and $G(T)$ are given by

$$R'(z) = \sum_k k r_k z^{k-1},$$

$$G(T) = R'(1 - T_n^{m-1}) [H(T_n) - Q'(T_n)]. \quad (53)$$

Using the mathematical identities listed above and using a procedure similar to the one used for deriving the expression of the Jacobian, it can be shown that $\partial \mathbf{F}_n / \partial x$ is given by

$$\frac{\partial \mathbf{F}_n}{\partial x} = \begin{pmatrix} \langle k \rangle T_n 2[H(T_n) - Q'(T_n)] + \langle k \rangle [T_n Q'(T_n) - Q(T_n)] - 2(1-p)T_n G(T_n) \\ 2(1-p)T_n G(T_n) \\ (1-p)T_n G(T_n) \end{pmatrix}.$$

For $T_n < 1$ the Jacobian \mathbf{J}_n has the largest eigenvalue λ_n given by

$$\lambda_n = \frac{1}{2} \left[\sqrt{\hat{\Delta}(T_n)} + \hat{K}(T_n) \right], \quad (54)$$

where $\hat{\Delta}(T_n)$ and $\hat{K}(T_n)$ are given by

$$\begin{aligned} \hat{\Delta}(T_n) &= [\hat{K}(T_n)]^2 - 4(1-p)H(T_n)Q'(T_n)R'(1 - T_n^{m-1})\langle k \rangle, \\ \hat{K}(T_n) &= [2\langle k \rangle - (1-p)R'(1 - T_n^{m-1})]H(T_n) \\ &\quad - [\langle k \rangle - 2(1-p)R'(1 - T_n^{m-1})]Q'(T_n). \end{aligned} \quad (55)$$

For $T_n = 1$, instead, the largest eigenvalue is given by

$$\lambda_n = \langle k \rangle (m-1).$$

The eigenvector \mathbf{u}_n corresponding to the largest eigenvalue is

$$\mathbf{u}_n = \mathcal{C} \begin{pmatrix} \hat{K}(T_n) - 2(1-p)R'(1 - T_n^{m-1})H(T_n) + \sqrt{\hat{\Delta}(T_n)} \\ 4(1-p)R'(1 - T_n^{m-1})[H(T_n) - Q'(T_n)] \\ 2(1-p)R'(1 - T_n^{m-1})[H(T_n) - Q'(T_n)] \end{pmatrix},$$

where \mathcal{C} is the normalization constant. For $T_n = 1$ and $p = p_c$, the eigenvector \mathbf{u}_n is given by

$$\mathbf{u}_n = (1, 0, 0)^\top.$$

Finally by using Eqs. (4) and (47) we can determine the fractal exponent ψ starting from the explicit expression of the eigenvalue λ_n given by Eq. (54).

C. Critical scaling of the fractal exponent

Here we consider the critical scaling of the fractal exponent close to the upper percolation threshold in the case in which the critical percolation probability $T_c = 1$ is reached continuously by the solution of Eq. (10). When $T_c = 1$, by expanding $Q'(T_n)$ and $H(T_n)$ close to the critical point, i. e., for $p = p_c + \Delta p$, and $T_n = T_c + \Delta T_n$ for

$\Delta p < 0$ and $\Delta T_n < 0$ but small in absolute values, i. e., $|\Delta T_n| \ll 1$ and $|\Delta p| \ll 1$, we obtain

$$\begin{aligned} Q'(T_n) &= (m-1) + (m-1)(m-2)\Delta T_n + \\ &\quad \frac{1}{2}(m-1)(m-2)(m-3)(\Delta T_n)^2 + o((\Delta T_n)^2), \\ H(T_n) &= (m-1) + \frac{1}{2}(m-1)(m-2)\Delta T_n \\ &\quad + \frac{1}{6}(m-1)(m-2)(m-3)(\Delta T_n)^2 + o((\Delta T_n)^2). \end{aligned}$$

Moreover we can also expand the expression $R'(1 - T_n^{m-1})$ obtaining

$$\begin{aligned} R'(1 - T_n^{m-1}) &\simeq r_1 - 2r_2(m-1)\Delta T_n \\ &\quad + [-r_2(m-1)(m-2) + 3r_3(m-1)^2](\Delta T_n)^2 + o((\Delta T_n)^2). \end{aligned}$$

By using the definition of ψ_n (Eq. (47)) and the explicit expression of λ_n (Eq. (54)) we can derive the scaling of ψ_n as a function of ΔT_n

$$\psi_n \simeq 1 - a(\Delta T_n)^2 \quad (56)$$

where a is a constant given by

$$\begin{aligned} a &= \frac{(m-2)}{[6\langle k \rangle^2(m-1) - 6] \ln[\langle k \rangle(m-1)]} \\ &\quad \times [\langle k \rangle^2(m-3)(m-1) + 2m-3] \end{aligned}$$

Therefore, for the branching cell complexes considered in this work, as long as the critical percolation probability $T_c = 1$ is reached continuously by the solution of Eq. (7), the critical scaling of ψ_n is universally dictated by Eq. (56) (note however that this critical behavior can be altered if the size of the polygons m is randomly distributed and its distribution is fat-tailed [13]). From the universal scaling of ψ_n as a function of ΔT_n we can derive the critical behavior of the fractal exponent as a function of ΔT by performing the limit $n \rightarrow \infty$. In Sec. III we have shown that the scaling of ΔT with Δp can be characterized by any exponent of the type $\beta = 1/(s-1)$ when

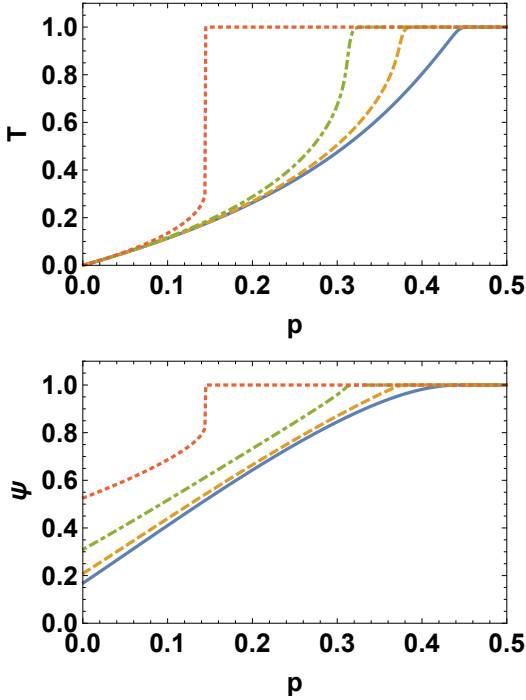


FIG. 7. The percolation probability T and the fractional exponent ψ are plotted as a function of occupation probability p of the links. Here we consider a branching simplicial complex ($m = 3$) with r_k distribution $r_k = r_1\delta_{k,1} + r_2\delta_{k,2} + r_3\delta_{k,3}$ with (r_1, r_2, r_3) given by $(0.9, 0.05, 0.05)$ for the solid blue line (continuous critical point of Eq. (10)), $(0.8, 0.2, 0)$ for the orange dashed line (tricritical point of Eq. (10)), $(0.727273, 0.181818, 0.0909091)$ for the green dot-dashed line (s order critical point of Eq. (10) with $s = 4$) and $(0.15, 0.54, 0.31)$ for the red dotted line (discontinuous critical point of Eq. (10)).

$T_c = 1$ is reached continuously. This implies that the fractal exponent scales like

$$\psi \simeq 1 - \tilde{a}(\Delta p)^{2\beta}, \quad (57)$$

where \tilde{a} is a constant. For the topologies considered in this work the only possible deviation from the universal critical scaling ψ_n as a function of ΔT_n given by Eq. (56) is observed when at the upper percolation threshold the percolation probability is discontinuous. In this case we will also observe a discontinuity of the fractal exponent ψ at p_c . In Fig. 7 we display the percolation probability T as a function of p for branching cell complexes undergoing percolation transitions of different universality classes at the upper percolation threshold $p = p_c$.

IX. ORDER PARAMETER

A. General framework

In this section we use the RG technique [13, 40] to predict the nature of the percolation phase transition at

the upper critical percolation threshold p_c . At p_c the order parameter is given by the fraction P_∞ of nodes in the giant component in an infinite network given by Eq. (5), which we rewrite here for convenience,

$$P_\infty = \lim_{n \rightarrow \infty} \frac{M_n}{N_n}. \quad (58)$$

By using Eq. (46) for approximating M_n when $n \gg 1$ we obtain

$$P_\infty \simeq \lim_{n \rightarrow \infty} \frac{1}{N_n^{(0)}} \prod_{n'=1}^n \lambda_{n'} \simeq \exp \left[-\ln[\langle k \rangle (m-1)] \int_0^\infty dn(1 - \psi_n) \right]. \quad (59)$$

The RG flow can be derived directly by the RG Eq. (6), which we rewrite here for convenience as

$$T_{n+1} = F(p, T_n) = 1 - (1-p) \sum_k r_k (1 - T_n^{m-1})^k \quad (60)$$

In the RG procedure one proceeds as follows.

First, the RG equation (60) is expanded close to the critical point $(p, T) = (p_c, T_c)$, obtaining the scaling of $\Delta T_n = T_n - T_c$ with n , for $0 < \Delta p = p - p_c \ll 1$. Secondly, this scaling is inserted in Eq. (56) characterizing the critical behavior of $1 - \psi_n$ as a function of ΔT_n . Finally, using Eq. (59), we can predict the nature of the phase transition by deriving the scaling of the order parameter P_∞ close to the upper percolation threshold. Here we conduct this RG study in the different phases of percolation defined on branching cell complexes and we explain the different critical behavior that can be observed for the percolation order parameter P_∞ (see Fig. 8).

In the following sections we will use the RG technique to predict that at the transcritical bifurcation point the percolation transition is discontinuous, similar to the Farey graph [32] and well-behaved generalized 2d hyperbolic manifolds [13]; at the saddle-node bifurcation point we predict a BKT transition and at the third-order pitchfork bifurcation point we predict a second-order critical behavior (see Fig. 8). These results confirm and generalize previous results obtained in hierarchical networks and specifically the flower network [36–38, 40]. Here we reveal additional universality classes that can occur at the pitchfork singularities of order $s > 3$ where we predict and observe a critical scaling of the type

$$P_\infty \simeq \exp[-\mathcal{A}/(\Delta p)^\sigma] \quad (61)$$

with the theoretically derived anomalous exponent $\sigma = (s-3)/(s-1)$.

B. RG theory at the transcritical bifurcation point

At the transcritical bifurcation point we observe a discontinuous percolation transition that is in the same universality class as percolation in the Farey graph [32] and

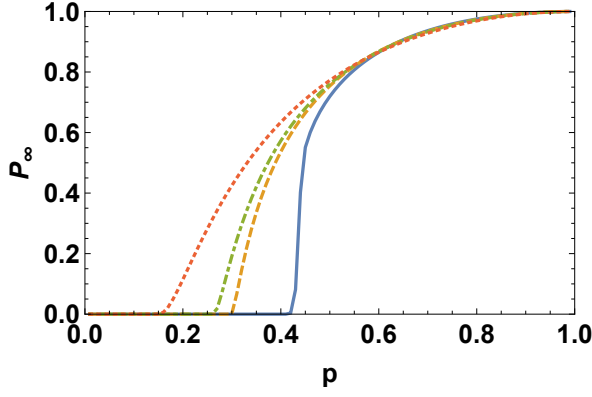


FIG. 8. The percolation order parameter P_∞ as a function of occupation probability p of the links. Here we consider a branching simplicial complex ($m = 3$) with r_k distribution $r_k = r_1\delta_{k,1} + r_2\delta_{k,2} + r_3\delta_{k,3}$ with (r_1, r_2, r_3) given by $(0.9, 0.05, 0.05)$ for the solid blue line (discontinuous percolation transition), $(0.8, 0.2, 0)$ for the orange dashed line (second-order transition), $(0.727273, 0.181818, 0.0909091)$ for the green dot-dashed line (anomalous transition following Eq. (61) with $\sigma = 3$) and $(0.15, 0.54, 0.31)$ for the red dotted line (BKT transition). The figure has been obtained by iterating Eq. (42) for $n = 1000$ iterations.

in well-behaved $2d$ cell complexes [13]. The derivation of this result follows steps similar to the ones previously reported in Ref. [13]. Here we report these results for the self-consistency of this work.

Our goal is to study the critical behavior above the upper percolation threshold, for $\Delta p = p - p_c > 0$. We expand the RG equation (60) for $0 < \Delta p \ll 1$ and $|\Delta T_n| = |T - T_c| \ll 1$ when $p_c = 1 - 1/[(m-1)r_1]$ and $T_c = 1$ obtaining

$$\begin{aligned} T_{n+1} = F(p_c, T_c) &+ \left. \frac{\partial F}{\partial p} \right|_{p=p_c, T=T_c} \Delta p \\ &+ \left. \frac{\partial F}{\partial T} \right|_{p=p_c, T=T_c} \Delta T_n + \left. \frac{\partial^2 F}{\partial p \partial T} \right|_{p=p_c, T=T_c} \Delta p \Delta T_n \\ &+ \frac{1}{2} \left. \frac{\partial^2 F}{\partial T^2} \right|_{p=p_c, T=T_c} (\Delta T_n)^2 + \dots \end{aligned} \quad (62)$$

with

$$F(p_c, T_c) = T_c = 1,$$

$$\left. \frac{\partial F}{\partial p} \right|_{p=p_c, T=T_c} = 0, \quad (63)$$

$$\left. \frac{\partial F}{\partial T} \right|_{p=p_c, T=T_c} = 1, \quad (64)$$

$$\left. \frac{\partial^2 F}{\partial p \partial T} \right|_{p=p_c, T=T_c} = -r_1(m-1), \quad (65)$$

$$\left. \frac{\partial^2 F}{\partial T^2} \right|_{p=p_c, T=T_c} = \frac{r_1(m-2) - 2r_2(m-1)}{r_1} \quad (66)$$

$$(67)$$

Therefore by truncating the expansion to the leading terms in ΔT_n and Δp we can write

$$\Delta T_{n+1} - \Delta T_n = \hat{C} \Delta T_n [\Delta T_n - \hat{B} \Delta p], \quad (68)$$

with constants \hat{B} and \hat{C} given by

$$\hat{B} = \frac{2(m-1)r_1^2}{(m-2)r_1 - 2r_2(m-1)}, \quad (69)$$

$$\hat{C} = \frac{1}{2r_1} [(m-2)r_1 - 2r_2(m-1)]. \quad (70)$$

For $n \rightarrow \infty$, we adopt a continuous approximation of Eq. (68). We indicate with x the continuous approximation of $-\Delta T_n \ll 1$, i.e., $x \simeq -\Delta T_n$, that follows the differential equation

$$\frac{dx}{dn} = -\hat{C}x[x + \hat{B}\Delta p], \quad (71)$$

with initial condition $x(0) = 1 - p$. This equation has the solution

$$x(n) = \hat{B}\Delta p \left[\left(1 + \frac{\hat{B}\Delta p}{1-p} \right) e^{\hat{C}\hat{B}\Delta p n} - 1 \right]^{-1}. \quad (72)$$

For $r_1 > 2r_2(m-1)/(m-2)$, ψ_n obeys the scaling relation Eq. (56) that can be expressed as a function of $x(n)$ as

$$\psi_n = 1 - a(T_c - T_n)^2 = 1 - a[x(n)]^2. \quad (73)$$

Consequently, using Eq. (59) we can express P_∞ in the continuous approximation as

$$P_\infty(p) \simeq \exp \left[-\ln[\langle k \rangle (m-1)] a \int dn [x(n)]^2 \right]. \quad (74)$$

Using the expression of $x(n)$ given by Eq. (72) we obtain for $0 < p - p_c \ll 1$

$$\begin{aligned} P_\infty(p) \simeq \exp \left[-\ln[\langle k \rangle (m-1)] a \left(\frac{(1-p)}{\hat{C}} \right. \right. \\ \left. \left. + \frac{\hat{B}\Delta p}{\hat{C}} \ln \left(\frac{\hat{B}\Delta p}{\hat{C}} \right) \right) \right] \end{aligned} \quad (75)$$

which can also be written as

$$P_\infty(p) \simeq P_\infty(p_c) \left(\frac{\Delta p}{r} \right)^{-h\Delta p} \quad (76)$$

where $P_\infty(p_c)$, h and r are given by

$$P_\infty(p_c) = \exp \left[-\ln[\langle k \rangle (m-1)] a \frac{2}{(m-1)(m-2)} \right],$$

$$h = \ln[\langle k \rangle (m-1)] a \frac{\hat{B}}{\hat{C}},$$

$$r = \frac{\hat{C}}{\hat{B}(m-1)}. \quad (77)$$

Eq. (76) can be further expanded for $0 < \Delta p \ll 1$ obtaining the critical behavior

$$P_\infty(p) \simeq P_\infty(p_c) + \alpha \Delta p [-\ln(\Delta p)], \quad (78)$$

where $\alpha = P_\infty(p_c)h$.

C. RG theory at the saddle-node bifurcation point

In this section we follow Ref. [38, 40] and by using the RG theory we show that as long as $T_c < 1$ the upper percolation threshold follows a BKT transition. Developing Eq. (60) for $T_n = T_c + \Delta T_n$ and $p = p_c + \Delta p$ with $0 < \Delta p \ll 1$ up to second order we obtain

$$T_{n+1} \simeq F(p_c, T_c) + \left. \frac{\partial F}{\partial p} \right|_{p=p_c, T=T_c} \Delta p + \left. \frac{\partial F}{\partial T} \right|_{p=p_c, T=T_c} \Delta T_n + \frac{1}{2} \left. \frac{\partial^2 F}{\partial T^2} \right|_{p=p_c, T=T_c} (\Delta T_n)^2,$$

with

$$F(p_c, T_c) = T_c < 1, \quad \left. \frac{\partial F}{\partial p} \right|_{p=p_c, T=T_c} = a = \frac{1 - T_c}{1 - p_c} > 0, \quad (79)$$

$$\left. \frac{\partial F}{\partial T} \right|_{p=p_c, T=T_c} = 1, \quad (80)$$

$$\left. \frac{\partial^2 F}{\partial T^2} \right|_{p=p_c, T=T_c} = 2b > 0. \quad (81)$$

$$(82)$$

Therefore close to the upper percolation transition ΔT_n evolves according to the equation

$$\Delta T_{n+1} - \Delta T_n = a\Delta p + b(\Delta T_n)^2. \quad (83)$$

For $|\Delta T_n| \ll 1$ we can write the above equation in the continuous limit as

$$\frac{dy(\hat{n})}{d\hat{n}} = 1 + y^2, \quad (84)$$

where $\hat{n} = n\delta$ and $\delta = \sqrt{ab\Delta p}$ and $y = b\Delta T_n/\delta$. This equation has the solution

$$y(\hat{n}) = \tan(\hat{n} + \tan^{-1}[y(0)]), \quad (85)$$

displaying a divergence for $\hat{n}_c = n_c\delta$ such that $\hat{n}_c + \tan^{-1}(y(0)) = \pi/2$. Therefore, the continuous approximation of ΔT_n indicated by $x(n)$ obeys

$$x(n) = \frac{\delta}{b} \tan(n\delta + \tan^{-1}[y(0)]). \quad (86)$$

The initial condition $x(0) = (T_0 - T_c) \leq 0$ implies that $y(0) \leq 0$. However, the function $x(n)$ eventually becomes positive and diverges for $n = n_c = \hat{n}_c/\delta$. At $n_c \simeq \hat{n}_c/\delta$ the approximation $x(n) \ll 1$ is no longer valid and the solution $x(n)$ has a jump to the trivial solution $x_0 = 1 - T_c$. In the latter case, we have that $1 - \psi_n$ will also have a discontinuity at n_c (see Fig. 9), i.e.,

$$1 - \psi_n = \begin{cases} f_\psi(\hat{n}) & \text{for } n < n_c \\ 0 & \text{for } n > n_c \end{cases}. \quad (87)$$

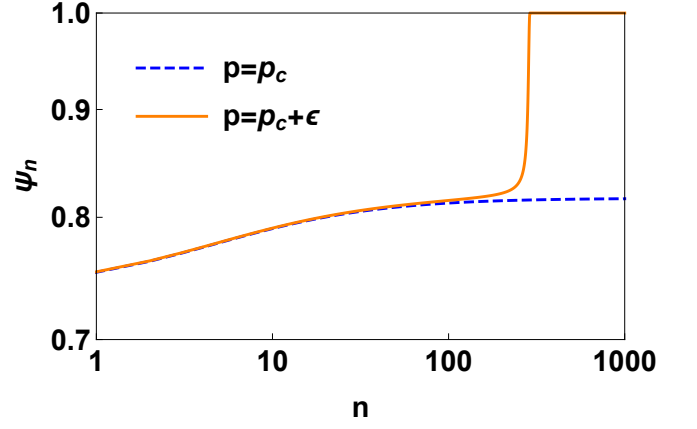


FIG. 9. The scaling of the exponent ψ_n as a function of n is plotted at the critical point $p = p_c$ corresponding to the BKT transition and slightly above the critical point for $p = p_c + \epsilon$ with $\epsilon = 10^{-4}$. The r_k distribution is given by $r_k = 0.1\delta_{k,1} + 0.5\delta_{k,2} + 0.3\delta_{k,3} + 0.1\delta_{k,4}$ and $p_c = 0.1261(7)$.

Therefore, the critical transition is continuous and follows the BKT singularity. In fact we have

$$P_\infty \simeq \exp \left[- \int_0^\infty dn(1 - \psi_n) \right] \simeq \exp \left[- \frac{1}{\delta} \int_0^{\hat{n}_c} d\hat{n} f_\psi(\hat{n}) \right] \simeq \exp \left[- \frac{\alpha}{\sqrt{\Delta p}} \right], \quad (88)$$

where α is a constant. This BKT transition has already been reported for specific branching cell complexes and other 2d hierarchical networks in Refs. [36–38] and in 3d hyperbolic manifolds in Ref. [12].

D. RG theory at the pitchfork bifurcation points

In this section we study the nature of the percolation transition of the pitchfork bifurcation points. We start with the treatment of the tricritical point of Eq. (10), finding that in this case the transition is second order and subsequently we discuss the case of critical points of order $s > 3$ of Eq. (10) finding continuous phase transitions with anomalous critical behavior.

Let us expand the RG equation (60) close to the tricritical point (p_c, T_c) for $0 < \Delta p \ll 1$ and $|\Delta T_n| \ll 1$ when $r_1 = 2r_2(m-1)/(m-2)$, $p_c = 1 - 1/[(m-1)r_1]$

and $T_c = 1$. In this way we obtain

$$\begin{aligned}
T_{n+1} \simeq & F(p_c, T_c) + \frac{\partial F}{\partial p} \Big|_{p=p_c, T=T_c} \Delta p \\
& + \frac{\partial F}{\partial T} \Big|_{p=p_c, T=T_c} \Delta T_n + \frac{\partial^2 F}{\partial p \partial T} \Big|_{p=p_c, T=T_c} \Delta p \Delta T_n \\
& + \frac{1}{2} \frac{\partial^2 F}{\partial T^2} \Big|_{p=p_c, T=T_c} (\Delta T_n)^2 \\
& + \frac{1}{6} \frac{\partial^3 F}{\partial T^3} \Big|_{p=p_c, T=T_c} (\Delta T_n)^3,
\end{aligned} \tag{89}$$

with

$$F(p_c, T_c) = T_c = 1,$$

$$\frac{\partial F}{\partial p} \Big|_{p=p_c, T=T_c} = 0, \tag{90}$$

$$\frac{\partial F}{\partial T} \Big|_{p=p_c, T=T_c} = 1, \tag{91}$$

$$\frac{\partial^2 F}{\partial p \partial T} \Big|_{p=p_c, T=T_c} = -r_1(m-1), \tag{92}$$

$$\frac{\partial^2 F}{\partial T^2} \Big|_{p=p_c, T=T_c} = 0, \tag{93}$$

$$\frac{\partial^3 F}{\partial T^3} \Big|_{p=p_c, T=T_c} < 0. \tag{94}$$

Therefore, by truncating the expansion to the leading terms in ΔT_n and Δp we can write

$$\Delta T_{n+1} - \Delta T_n = -\hat{C} \Delta T_n \left[(\Delta T_n)^2 + \hat{B} \Delta p \right], \tag{95}$$

where constants \hat{B} and \hat{C} are given by

$$\hat{B} = \frac{r_1(m-1)}{\hat{C}}, \tag{96}$$

$$\hat{C} = -\frac{1}{6} \frac{\partial^3 F}{\partial T^3} \Big|_{p=p_c, T=T_c}. \tag{97}$$

For $n \rightarrow \infty$ we approximate the above equation in the continuous limit and we use x to indicate the continuous approximation of $-\Delta T_n \ll 1$, i.e., $x \simeq -\Delta T_n$. In this way we get the differential equation

$$\frac{dx}{dn} = -\hat{C} x [x^2 + \hat{B} \Delta p], \tag{98}$$

with initial condition $x(0) = 1 - p$, whose solution is

$$x(n) = \sqrt{\hat{B} \Delta p} \left[\left(1 + \frac{\hat{B} \Delta p}{(1-p)^2} \right) e^{2\hat{C} \hat{B} \Delta p n} - 1 \right]^{-1/2} \tag{99}$$

Therefore the percolation order parameter P_∞ is given by

$$\begin{aligned}
P_\infty(p) & \simeq \exp \left[-\ln[\langle k \rangle (m-1)] a \int_0^\infty [x(n)]^2 \right] \\
& \simeq \left(\frac{\hat{B} \Delta p}{(1-p)^2} \right)^{\hat{\beta}} \propto (\Delta p)^{\hat{\beta}},
\end{aligned} \tag{100}$$

where

$$\hat{\beta} = \ln[\langle k \rangle (m-1)] \frac{a}{2\hat{C}}. \tag{101}$$

It follows that in this case the transition is continuous with a critical exponent $\hat{\beta}$. This phase transition has been reported in the case of the flower network in Ref. [38].

At the higher-order critical points of Eq. (10) of order s we have

$$F(p_c, T_c) = T_c = 1,$$

$$\frac{\partial F}{\partial p} \Big|_{p=p_c, T=T_c} = 0, \tag{102}$$

$$\frac{\partial F}{\partial T} \Big|_{p=p_c, T=T_c} = 1, \tag{103}$$

$$\frac{\partial^2 F}{\partial p \partial T} \Big|_{p=p_c, T=T_c} = -r_1(m-1), \tag{104}$$

$$\frac{\partial^j F}{\partial T^j} \Big|_{p=p_c, T=T_c} = 0, \tag{105}$$

$$(-1)^s \frac{\partial^s F}{\partial T^s} \Big|_{p=p_c, T=T_c} > 0, \tag{106}$$

for $j = 1, 2, \dots, (s-1)$. Therefore by expanding the RG equation (60) close to the s -critical point (p_c, T_c) for $0 < \Delta p \ll 1$ and $|\Delta T_n| \ll 1$ when $r_1 = 2r_2(m-1)/(m-2)$, $p_c = 1 - 1/[(m-1)r_1]$ and $T_c = 1$ up to order s we get

$$\begin{aligned}
T_{n+1} \simeq & F(p_c, T_c) + \frac{\partial F}{\partial p} \Big|_{p=p_c, T=T_c} \Delta p \\
& + \frac{\partial F}{\partial T} \Big|_{p=p_c, T=T_c} \Delta T_n + \frac{\partial^2 F}{\partial p \partial T} \Big|_{p=p_c, T=T_c} \Delta p \Delta T_n \\
& + \frac{1}{s!} \frac{\partial^s F}{\partial T^s} \Big|_{p=p_c, T=T_c} (\Delta T_n)^s.
\end{aligned} \tag{107}$$

Therefore, by truncating the expansion to the leading terms in ΔT_n and Δp we can write

$$\Delta T_{n+1} - \Delta T_n = -\hat{C} \Delta T_n \left[(-1)^{s-1} (\Delta T_n)^{s-1} + \hat{B} \Delta p \right],$$

where constants \hat{B} and \hat{C} are given by

$$\hat{B} = \frac{r_1(m-1)}{\hat{C}}, \tag{108}$$

$$\hat{C} = (-1)^s \frac{1}{s!} \frac{\partial^s F}{\partial T^s} \Big|_{p=p_c, T=T_c}. \tag{109}$$

By performing the limit $n \rightarrow \infty$ we can derive the equation for the continuous approximation of $-\Delta T_n \ll 1$, indicated as $x(n)$, i.e., $x \simeq -\Delta T_n$. This equation reads

$$\frac{dx}{dn} = -\hat{C} x [x^{s-1} + \hat{B} \Delta p], \tag{110}$$

with initial condition $x(0) = 1 - p$. This equation has

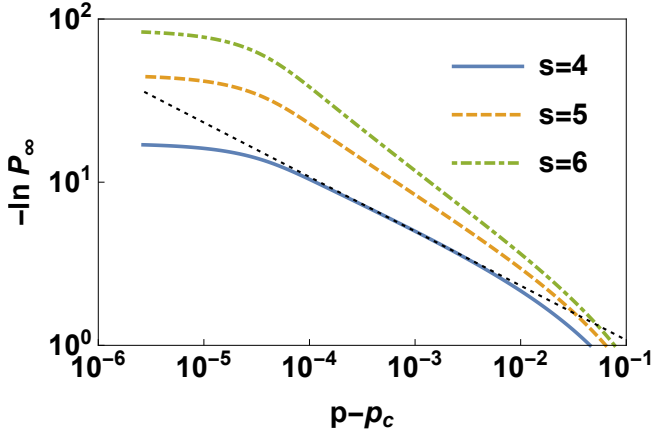


FIG. 10. The critical scaling of the order parameter P_∞ versus $p - p_c$ is shown for branching simplicial complexes ($m = 3$) with distribution $r_k = r_1\delta_{k,1} + r_2\delta_{k,2} + r_3\delta_{k,3} + r_4\delta_{k,4} + r_5\delta_{k,5}$ and parameter values corresponding to the critical points of order s of Eq. (10). Here the data are obtained by iterating Eq. (42) $n = 2 \cdot 10^4$ times. The thin dotted line is the theoretically predicted scaling given by Eq. (61) with $\sigma = 1/3$.

the solution

$$x(n) = (\hat{B}\Delta p)^\gamma \left[\left(1 + \frac{\hat{B}\Delta p}{(1-p)^{s-1}} \right) e^{(s-1)\hat{C}\hat{B}\Delta p n} - 1 \right]^{-\gamma},$$

with $\gamma = 1/(s-1)$. Therefore the fraction of nodes in the giant component can be approximated by

$$\begin{aligned} P_\infty(p) &\simeq \exp \left[-\ln[\langle k \rangle (m-1)] a \int_0^\infty [x(n)]^2 \right] \\ &\simeq \exp [-\mathcal{A}(\Delta p)^{-\sigma}], \end{aligned} \quad (111)$$

where \mathcal{A} is a constant and $\sigma = (s-3)/(s-1)$. Therefore the transition is continuous with a non-trivial singularity dictated by the exponent σ which can in general be different from $\sigma = 1$ and $\sigma = 1/2$. This expression reduces to the BKT singularity for $s = 5$, i.e., $P_\infty(p) \propto \exp[-\mathcal{A}/\sqrt{\Delta p}]$ and in the limit $s \rightarrow \infty$ reduces to the scaling $P_\infty(p) \propto \exp[-\mathcal{A}/\Delta p]$, but in general might be non-trivial. To our knowledge this anomalous critical scaling has not been reported previously for any specific branching cell complex.

Here we compare the RG predictions with extensive simulations for critical points of Eq. (10) of order $s = 4, 5, 6$ (see Fig. 10). We have found evidence that the

exponent σ grows with the order s of the critical point as predicted by the continuous RG approach. For $s = 4$ we found a perfect agreement with the theoretical prediction $\sigma = 1/3$. However for $s = 5, 6$ the exponent that we found numerically slightly differs from the predictions. This deviation from the theoretical predictions could be an effect of finite sizes or also due to the continuous approximation that we have used to predict the critical scaling.

X. CONCLUSIONS

In this work we have investigated the relation between network geometry and dynamics on branching simplicial and cell complexes. Our main results are two-fold. On the one hand, we have shown that the discontinuous percolation transition is observed not only in hyperbolic manifolds but also in branched non-amenable hierarchical networks. In this way we have generalized previous results restricted to special cases of branching simplicial complexes. Additionally, we have shown that, as the topology of the branched cell complex is evolving, the upper percolation transition can display non-trivial continuous critical behavior. On the other hand, we have shown that the considered non-amenable networks can have a number of intermediate phase transitions besides the upper and the lower one. At the lower percolation transition, the percolation probability becomes larger than zero but the giant component is not extensive. At the upper percolation transition the giant component becomes extensive. At the intermediate phase transitions the percolation probability and the fractal exponent have abrupt discontinuities but the fractal exponents remain smaller than one. Therefore below and above these intermediate phase transitions the giant component remains sub-extensive. The latter result was derived by exploiting the mathematical similarities between the equations determining the percolation probability of simplicial and cell complexes with the equations determining the emergence of the MCGC in correlated multiplex networks. Despite the fact that the relation between the two percolation problems appears to be only a formal one, we expect that this result might be useful to further stimulate the research on the universal properties of explosive percolation problems. Namely, this work can be extended in several directions, including, for instance, the treatment of higher-dimensional simplicial and cell complexes and the case in which the 2-dimensional cell complexes are formed by m -polygons with heterogeneous distribution for the number of faces m .

-
- [1] S. N. Dorogovtsev, A. V. Goltsev, and J. F. Mendes, *Rev. Mod. Phys.* **80**, 1275 (2008).
 - [2] A.-L. Barabási *et al.*, *Network science* (Cambridge university press, 2016).

- [3] S. N. Dorogovtsev and J. F. Mendes, *Evolution of networks: From biological nets to the Internet and WWW* (OUP Oxford, 2013).
- [4] G. Bianconi, *Multilayer Networks: Structure and Function* (Oxford University Press, Oxford, 2018).

- [5] S. Boccaletti, G. Bianconi, R. Criado, C. I. Del Genio, J. Gómez-Gardenes, M. Romance, I. Sendina-Nadal, Z. Wang, and M. Zanin, *Phys. Rep.* **544**, 1 (2014).
- [6] M. Kivelä, A. Arenas, M. Barthélemy, J. P. Gleeson, Y. Moreno, and M. A. Porter, *Jour. Com. Net.* **2**, 203 (2014).
- [7] G. Bianconi, *EPL (Europhys. Lett.)* **111**, 56001 (2015).
- [8] V. Salnikov, D. Cassese, and R. Lambiotte, *Euro. J. Phys.* **40**, 014001 (2018).
- [9] G. Bianconi and C. Rahmede, *Sci. Rep.* **7**, 41974 (2017).
- [10] G. Bianconi and C. Rahmede, *Phys. Rev. E* **93**, 032315 (2016).
- [11] D. Mulder and G. Bianconi, *J. Stat. Phys.* **173**, 783 (2018).
- [12] G. Bianconi and R. M. Ziff, *Phys. Rev. E* **98**, 052308 (2018).
- [13] I. Kryven, R. M. Ziff, and G. Bianconi, *Phys. Rev. E* **100**, 022306 (2019).
- [14] A. P. Millán, J. J. Torres, and G. Bianconi, *Sci. Rep.* **8**, 9910 (2018).
- [15] A. P. Millán, J. J. Torres, and G. Bianconi, *Phys. Rev. E* **99**, 022307 (2019).
- [16] M. Šuvakov, M. Andjelković, and B. Tadić, *Sci. Rep.* **8**, 1987 (2018).
- [17] I. Iacopini, G. Petri, A. Barrat, and V. Latora, *Nat. Comm.* **10**, 2485 (2019).
- [18] P. S. Skardal and A. Arenas, *Phys. Rev. Lett.* **122**, 248301 (2019).
- [19] N. Araújo, P. Grassberger, B. Kahng, K. Schrenk, and R. Ziff, *Euro. Phys. J., Special Topics* **223**, 2307 (2014).
- [20] D. Lee, B. Kahng, Y. Cho, K.-I. Goh, and D.-S. Lee, *J. Korean Phys. Soc.* **73**, 152 (2018).
- [21] R. M. D'Souza, J. Gómez-Gardeñes, J. Nagler, and A. Arenas, *arXiv preprint arXiv:1907.09957* (2019).
- [22] D. Achlioptas, R. M. D'Souza, and J. Spencer, *Science* **323**, 1453 (2009).
- [23] O. Riordan and L. Warnke, *Science* **333**, 322 (2011).
- [24] R. A. da Costa, S. N. Dorogovtsev, A. V. Goltsev, and J. F. F. Mendes, *Phys. Rev. Lett.* **105**, 255701 (2010).
- [25] R. M. Ziff, *Phys. Rev. Lett.* **103**, 045701 (2009).
- [26] G. Bianconi, *Phys. Rev. E* **97**, 022314 (2018).
- [27] S. V. Buldyrev, R. Parshani, G. Paul, H. E. Stanley, and S. Havlin, *Nature* **464**, 1025 (2010).
- [28] R. Parshani, S. V. Buldyrev, and S. Havlin, *Phys. Rev. Lett.* **105**, 048701 (2010).
- [29] G. Baxter, S. Dorogovtsev, A. Goltsev, and J. Mendes, *Phys. Rev. Lett.* **109**, 248701 (2012).
- [30] I. Kryven, *Nat. Comm.* **10**, 404 (2019).
- [31] G. Bianconi and S. N. Dorogovtsev, *Phys. Rev. E* **89**, 062814 (2014).
- [32] S. Boettcher, V. Singh, and R. M. Ziff, *Nat. Comm.* **3**, 787 (2012).
- [33] H. Gu and R. M. Ziff, *Phys. Rev. E* **85**, 051141 (2012).
- [34] S. Mertens and C. Moore, *Phys. Rev. E* **96**, 042116 (2017).
- [35] D. M. Auto, A. A. Moreira, H. J. Herrmann, and J. S. Andrade Jr., *Phys. Rev. E* **78**, 066112 (2008).
- [36] S. Boettcher, J. L. Cook, and R. M. Ziff, *Phys. Rev. E* **80**, 041115 (2009).
- [37] T. Hasegawa, M. Sato, and K. Nemoto, *Phys. Rev. E* **82**, 046101 (2010).
- [38] T. Nogawa and T. Hasegawa, *Phys. Rev. E* **89**, 042803 (2014).
- [39] V. Singh and S. Boettcher, *Phys. Rev. E* **90**, 012117 (2014).
- [40] T. Nogawa, *J. Phys. A: Math. Gen.* **51**, 505003 (2018).
- [41] S. Boettcher and C. Brunson, *EPL (Europhysics Lett.)* **110**, 26005 (2015).
- [42] V. Singh, C. T. Brunson, and S. Boettcher, *Phys. Rev. E* **90**, 052119 (2014).
- [43] M. Hinczewski and A. N. Berker, *Phys. Rev. E* **73**, 066126 (2006).
- [44] S. N. Dorogovtsev, A. V. Goltsev, and J. F. F. Mendes, *Phys. Rev. E* **65**, 066122 (2002).
- [45] S. N. Dorogovtsev, *Phys. Rev. E* **67**, 045102 (2003).
- [46] I. Kryven and G. Bianconi, *Phys. Rev. E* **100**, 020301 (2019).
- [47] R. Lyons, *Jour. Math. Phys.* **41**, 1099 (2000).
- [48] A. A. Migdal, *Soviet Journal of Experimental and Theoretical Physics* **42**, 743 (1976).
- [49] L. P. Kadanoff, *Ann. Phys.* **100**, 359 (1976).